Temperature dependence of dark current properties of InGaAs/GaAs quantum dot solar cells

Hao Feng Lu,[1,a)] Lan Fu,[1] Greg Jolley,[1] Hark Hoe Tan,[1] Sudersena Rao Tatavarti,[2] and Chennupati Jagadish[1]
[1]*Department of Electronic Materials Engineering, Research School of Physics and Engineering, The Australian National University, Canberra ACT 0200, Australia*
[2]*MicroLink Devices, Inc., 6457 W. Howard St. Niles, Illinois 60714, USA*

(Received 22 March 2011; accepted 13 April 2011; published online 6 May 2011)

Self-assembled $In_{0.5}Ga_{0.5}As/GaAs$ quantum dot solar cell (QDSC) was grown by metal organic chemical vapor deposition. Systematic measurements of dark current versus voltage (I-V) characteristics were carried out from 30 to 310 K. Compared with the reference GaAs solar cell, the QDSC exhibits larger dark current however its ideality factor (n) was smaller, which cannot be straightly interpreted by the conventional diode models. These results are important for the fundamental understanding of QDSC properties and further implementation of new solar cell designs for improved efficiency. © *2011 American Institute of Physics*. [doi:10.1063/1.3586251]

Solar cells based on III–V compound semiconductors have attracted much research attention over the past several decades.[1] In order to make use of the low energy region (less than the band gap of GaAs) of solar spectrum, low dimensional structures have been introduced into III–V p-i-n structures, such as In(Ga)As quantum well[2,3] and quantum dots (QDs).[4–7] Many studies[8–11] indicate that incorporating QDs into the intrinsic region of a p-i-n solar cell can extend the photocurrent to longer wavelength, leading to a slightly increased short circuit current density. However, this is always accompanied by a reduction in the open circuit voltage (compared to the reference cells). Some investigations based on the study of current-voltage characteristics have been performed[12,13] to understand the effects of quantum structure on solar cell properties, however the dark current properties which are critical for the QD solar cell performance have not been studied in-depth previously. In this letter, we report on a detailed study of the temperature dependent dark current of InGaAs/GaAs QD solar cells.

The self-assembled $In_{0.5}Ga_{0.5}As/GaAs$ QD solar cell was grown on n^+-GaAs (001) substrate by metal organic chemical vapor deposition. In addition, a GaAs p-i-n cell was also grown as reference. The cells growth and structures have been described in detail.[14] Specifically, the intrinsic region of the QD solar cell consisted of ten $In_{0.5}Ga_{0.5}As$ QD layers (six monolayer each) sandwiched between 50 nm i-GaAs spacers. The dot density per layer is about 4.5×10^{10} cm^{-2}. The QD solar cell exhibits a strong photoluminescence peak at room temperature indicating high optical quality. For comparison, the GaAs reference cell has a 500 nm thick i-GaAs region. Both samples were fabricated into a few 1×1 mm^2 and 3×3 mm^2 square mesa devices with Au grids on the top surface of the device as p-type contact and Au/Ge on the back as n-type contact. After metallization the top 100 nm p^+ GaAs contact layer was removed by selective etching. The standard device parameters were measured by an Oriel solar simulator (AM1.5). Temperature dependent dark I-V characteristics were carried out in a close-cycled He cryostat. All devices were characterized without antireflection coatings.

The solar cell performance measurements were first performed under AM1.5 1 sun illumination. The GaAs control cell shows an open circuit voltage (V_{oc}) of 0.99 V, short circuit current density (J_{sc}) of 18.3 mA/cm^2, fill factor (FF) of 83.9%, and efficiency of 15.3% while the QD solar cell (QDSC) exhibits a slightly higher J_{sc} of 18.8 mA/cm^2, a reduced V_{oc} of 0.76 V, FF of 76.9%, and efficiency of 11.1%. These results are consistent with other studies on III–V QD systems.[6,15,16] For QD solar cells it has been expected that the absorption of low energy photons by the QD layers are able to make additional contribution to the photocurrent leading to some increase in the J_{sc}. Meanwhile the effects that lead to a reduction in the V_{oc} are found to be the injection of carriers from n- and p-type layers into the depletion region where they recombine with carriers occupying QD states due to quasithermal distribution.[14]

As shown in Fig. 1(a), the GaAs reference cell displays a steady increase in dark current with temperature, mainly as a

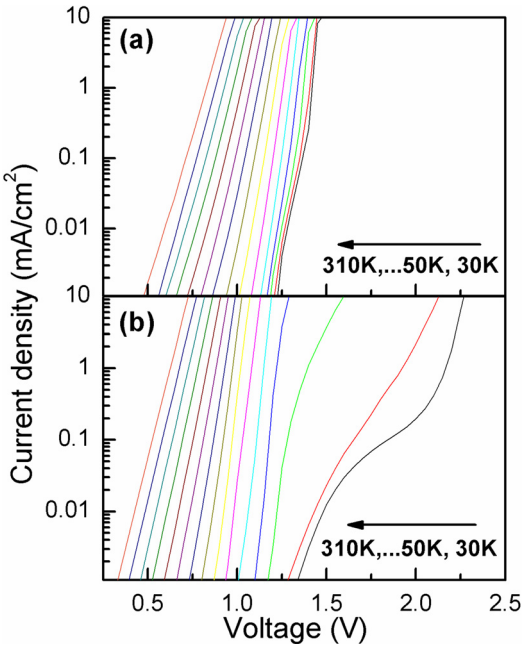

FIG. 1. (Color online) Temperature dependence dark J-V characteristics of (a) GaAs solar cell and (b) QD solar cell.

[a)]Electronic mail: hfl109@physics.anu.edu.au.

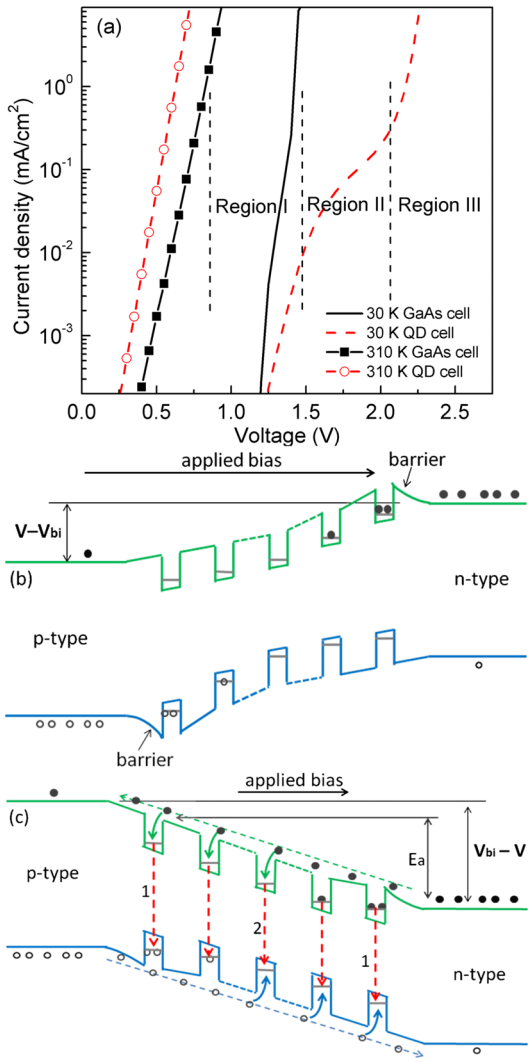

FIG. 2. (Color online) (a) Dark I-V characteristics of the solar cell devices measured at 30 and 300 K. Schematics demonstrating the different carrier capture and recombination behavior for QD solar cell devices at (b) low temperature (<70 K) and high bias condition ($V > V_{bi}$) and (c) high temperature (>70 K).

result of the exponential temperature dependence of the intrinsic carrier concentration n_i in the depletion region.[17] The QD device exhibits more complicated behavior. At low temperatures, the QD cell has much smaller dark current than that of the reference cell, however, its dark current increases more rapidly with temperature and when the temperature is over 70 K, the dark current follows a trend similar to that of the reference cell. Generally, for a normal p-i-n solar cell, the dark current due to the forward bias carrier injection is a combined result of recombination current in the space charge region (SCR) and diffusion current through the SCR. The change in the shape of the dark I-V curves with temperature depends on the concentration of different types of defects present in the sample with different temperature dependent carrier capture cross sections and tunneling effects.[18] On the other hand, for the QD device, presence of QDs in the depletion region introduces additional recombination paths via QD states to contribute to dark current, the amount of which largely depends on the carrier capture and recombination processes under different biases and temperatures. Fig. 2(a) replots the dark I-V curves of both devices at 30 and 300 K. At 30 K, in the region I in Fig. 2(a), the dark current of both devices remains very small and does not show substantial increase until a large voltage is applied. This is because at low temperatures, the kinetic energy of forward injected carriers is too small to overcome the built-in potential (V_{bi}) of the p-i-n junction to form appreciable dark current until the forward voltage is increased to a value close to V_{bi}. [The V_{bi} for our GaAs reference cell is estimated to be ~1.36 eV at room temperature and ~1.5 eV at 30 K.Here we assume our QD solar cell has a similar V_{bi} due to the same doping scheme.] For the QD cell the current is even smaller due to an additional potential barrier formed by QD carrier occupation.[19] Those QD layers particularly close to the contacts will be occupied by carriers which will form an electrostatic barrier that inhibits the further injection of carriers. This effect as shown schematically in Fig. 2(b) suppresses dark current even at biases larger than the V_{bi} [region II in Fig. 2(a)] where a large increase in dark current is observed for the reference cell. If the bias is further increased beyond 2.0 V the potential barrier is overcome and the carriers start to be injected through the depletion region leading to a rapid increase in dark current [region III in Fig. 2(a)].

TABLE I. The fitting parameters for the dark I-V curves measured at 300 K.

Samples	J_s (A/cm^2)	R_s (Ω)	R_{sh} (Ω)	n
GaAs cell	2.08×10^{-11}	1.29	3.04×10^{9}	1.91
QD cell	1.39×10^{-10}	2.06	1.78×10^{9}	1.66

The case is different at higher temperatures for QD device, e.g., >70 K, the thermal energy of carriers in the contact layers may overcome both the potential barrier and the built-in potential. As the injected carriers pass through the depletion region, there is a high probability for them to be captured by the QD potential and recombine via two different paths as demonstrated in Fig. 2(c): (1) for the QD layers that are close to the quasineutral regions, the majority carriers from the contact layers occupy QD states under a quasithermal equilibrium distribution. Under forward bias, these QD layers may capture injected minority carriers leading to recombination; (2) for those QD layers that are unoccupied (both conduction and valence bands), simultaneous capture of an electron and a hole by the same QD layer may also occur with subsequent recombination. These two paths will cause a reduction in forward injection thermal activation energy (E_a) in the QDSC (Ref. 14) and increase in dark current, as observed in Fig. 1(b).

Log(I)-V curves of both devices at relatively high temperatures can be fitted well using the modified one-diode exponential characteristic equation,[20,21]

$$J = J_s\left\{\exp\left[\frac{q(V - JR_s)}{nkT}\right] - 1\right\}, \quad (1)$$

where V is the voltage across the device, J_s is the reverse saturation current density, R_s is the series resistance, n is the ideality factor, q is electron charge, and k is the Boltzmann constant. The fitting parameters for both solar cell devices at 300 K are listed in Table I. The shunt resistances are also calculated using the slope of reverse I-V curves before breakdown and provided in Table I. Compared with the reference cell, the QDSC exhibits a larger R_s and smaller R_{sh}. Its large saturation current suggests possible presence of high

density defect in the QD structures due to the strain driven self-assembled QD growth as well as increased probability of thermal generation of carriers due to the small band gap of QDs. However, surprisingly the n value of the QDSC turns out to be smaller than that of the reference cell, which is contradictory to the rest of the results. This could be due to the following reasons. For conventional solar cells, at relatively low bias conditions, the dark current is normally dominated by recombination occurs within the depletion region, which results in a smaller slope of dark log(I)-V curve and larger n value (than 1). For the case of the QDSC, recombination within QDs makes a large contribution to the dark current. However, we propose that the two different recombination paths within QD layers as mentioned earlier may have different contributions to the overall ideality factor of the QDSC. As demonstrated in Fig. 2(c), under quasithermal equilibrium state, the first few QD layers will be occupied by majority carriers, which may then recombine with the injected minority carriers via path (1). This process is very similar to the formation of dark current outside the SCR which requires the transport of only one type of charge carrier through the depletion region, giving a low ideality factor (~1). On the other hand, it is also likely that electrons and holes are simultaneously captured by the same QD layer and recombine directly via path (2). This process, however, is associated with the QD capture cross sections for electrons and holes and is similar to the defect related recombination in the depletion region of the common solar cells leading to larger ideality factor (~2). Apparently for the QDSC studied in our work, despite its larger dark current, the recombination in the first few QD layers contributes significantly to the dark current and consequently a smaller ideality factor than the reference cell. To date, this unusual reduction in ideality factor n of QDSC has not been reported and/or discussed before. It suggests that for QDSC, new physical model may need to be developed to describe and simulate its complicated recombination behavior.

To further study the effects of carrier recombination on n factor, the local value can be calculated by Eq. (2),[22]

$$n(V) = \frac{d(V/V_t)}{d[\ln(I)]}, \tag{2}$$

where V_t is the thermal voltage of 0.026 eV at 300 K. The n(V) of both devices with different sizes have been plotted in Fig. 3. Both types of devices show a change in n-factor with the voltage. In the low bias region, the n-factor is larger indicating dark current is dominated by recombination in SCR. With increase in bias, the n-factors reduce to the lowest value before a large increase due to the series resistance effect at high biases. It can be seen that the reference cells have larger n values than the QD solar cell. In addition, the n(V) curves for the reference cells show fluctuations and sometimes with the presence of "peaks" in the curve, which imply additional path(s) of recombination, such as edge recombination. This is in contrast to the QD devices where consistent results have been obtained for all the devices with different sizes. It suggests that similar to the dots-in-a-well devices,[22] use of InGaAs/GaAs QDs may be able to block lateral current flow to the device perimeter thereby reduce the edge recombination.

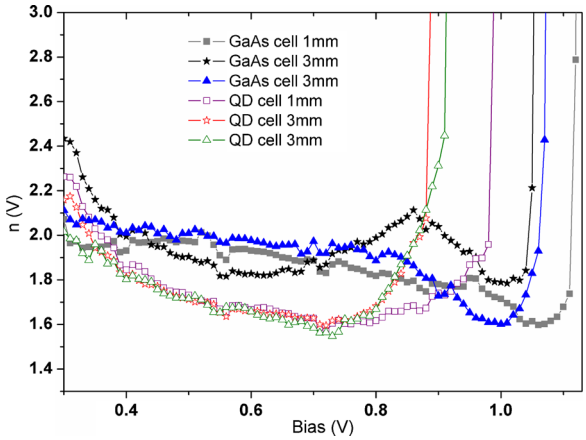

FIG. 3. (Color online) Voltage dependence of local ideality factor for various solar cell devices fabricated in this work.

In summary, the QD devices show complicated dark I-V behaviors due to temperature and bias dependent carrier capture, occupation and recombination. The results are critical for further development of new physical model for QDSCs.

The authors would like to acknowledge financial support from the Australian Research Council and facility support from the Australian National Fabrication Facility (ACT node). The authors also thank Prof. Andres Cuevas for important suggestions.

[1]M. A. Green, K. Emery, Y. Hishikawa, and W. Warta, Prog. Photovoltaics **17**, 320 (2009).
[2]M. Mazzer, K. W. J. Barnham, I. M. Ballard, A. Bessiere, A. Ioannides, D. C. Johnson, M. C. Lynch, T. N. D. Tibbits, J. S. Roberts, G. Hill, and C. Calder, Thin Solid Films **511**, 76 (2006).
[3]L. Z. Wu, W. Tian, and X. T. Jiang, J. Mater. Sci. **40**, 1451 (2005).
[4]D. Zhou, G. Sharma, S. F. Thomassen, T. W. Reenaas, and B. O. Fimland, Appl. Phys. Lett. **96**, 061913 (2010).
[5]A. Luque and A. Marti, Adv. Mater. (Weinheim, Ger.) **22**, 160 (2010).
[6]S. M. Hubbard, C. D. Cress, C. G. Bailey, R. P. Raffaelle, S. G. Bailey, and D. M. Wilt, Appl. Phys. Lett. **92**, 123512 (2008).
[7]Q. D. Zhuang, H. X. Li, L. Pan, J. M. Li, M. Y. Kong, and L. Y. Li, J. Cryst. Growth **201**, 1161 (1999).
[8]E. Antolin, A. Marti, C. R. Stanley, C. D. Farmer, E. Cánovas, N. López, P. G. Linares, and A. Luque, Thin Solid Films **516**, 6919 (2008).
[9]V. Aroutiounian, S. Petrosyan, A. Khachatryan, and K. Touryan, J. Appl. Phys. **89**, 2268 (2001).
[10]M. Y. Levy and C. Honsberg, J. Appl. Phys. **104**, 113103 (2008).
[11]A. Martí, E. Antolín, C. R. Stanley, C. D. Farmer, N. López, P. Díaz, E. Cánovas, P. G. Linares, and A. Luque, Phys. Rev. Lett. **97**, 247701 (2006).
[12]N. J. Ekins-Daukes, K. W. J. Barnham, J. P. Connolly, J. S. Roberts, J. C. Clark, G. Hill, and M. Mazzer, Appl. Phys. Lett. **75**, 4195 (1999).
[13]E. Aperathitis, C. G. Scott, D. Sands *et al.*, Adv. Technol. **51**, 85 (1998).
[14]G. Jolley, H. F. Lu, L. Fu, H. H. Tan, and C. Jagadish, Appl. Phys. Lett. **97**, 123505 (2010).
[15]V. Popescu, G. Bester, M. C. Hanna, A. G. Norman, and A. Zunger, Phys. Rev. B **78**, 205321 (2008).
[16]Y. Okada, R. Oshima, and A. Takata, J. Appl. Phys. **106**, 024306 (2009).
[17]E. Radziemska, Int. J. Energy Res. **30**, 127 (2006).
[18]R. Kachare, B. E. Anspaugh, and G. F. J. Garlick, Solid-State Electron. **31**, 159 (1988).
[19]V. Ryzhii, I. Khmyrova, V. Pipa, V. Mitin, and M. Willander, Semicond. Sci. Technol. **16**, 331 (2001).
[20]D. K. Schroder, *Semiconductor Material and Device Characterization*, 3rd ed. (Wiley, NJ, 2006), Chap. 4.
[21]N. Kavasoglu, A. S. Kavasoglu, and S. Oktik, Curr. Appl. Phys. **9**, 833 (2009).
[22]T. Y. Gu, M. A. El-Emawy, K. Yang, A. Stintz, and L. F. Lester, Appl. Phys. Lett. **95**, 261106 (2009).